Catalysis Today 155 (2010) 184–191

Contents lists available at ScienceDirect

Catalysis Today

journal homepage: www.elsevier.com/locate/cattod

DRIFTS-MS studies of preferential oxidation of CO in H_2 rich stream over $(CuO)_{0.7}(CeO_2)_{0.3}$ and $(Cu_{0.9}M_{0.1}O)_{0.7}(CeO_2)_{0.3}$ (M = Co, Zn and Sn) catalysts

Parthasarathi Bera, Aitor Hornés, Antonio López Cámara, Arturo Martínez-Arias *

Instituto de Catálisis y Petroleoquímica, CSIC, Campus Cantoblanco, 28049 Madrid, Spain

ARTICLE INFO

Article history:
Available online 18 September 2009

Keywords:
CO-PROX
XRD
Operando-DRIFTS-MS
CuO
CeO_2
Co
Zn
Sn

ABSTRACT

A series of catalysts based on combinations between copper and cerium oxides, in which the former has been modified by doping with Co, Zn and Sn, have been prepared by a microemulsion method and characterized by XRD and S_{BET} measurements. Their catalytic activity as well as details of redox processes taking place during the course of the reaction has been examined by means of *operando*-DRIFTS-MS under CO-PROX conditions. The results reveal differences in the characteristics of carbonyl species formed through a reductive process during the course of the reaction which are employed to rationalize catalytic properties of the systems.

1. Introduction

At present fuel cell technology is rapidly growing as a viable alternative source for sustainable energy generation and it has been used for both stationary and transportation applications [1]. It offers highly efficient conversion of chemical energy into electrical energy without emission of environmental pollutants, thereby making fuel cells one of the most promising sources of energy generation. Hydrogen is a clean fuel that emits no environmental pollutants when burned and is predicted to be a major source of energy in the future [2]. It has been found to be the most promising fuel for fuel cells. At this moment, proton-exchange membrane fuel cells (PEMFC) are most studied type of hydrogen based electrical power sources, both for static and mobile power applications. But H_2 has its own disadvantage due to the lack of infrastructure for its distribution and storage. Therefore, processing of fuels is necessary for producing H_2 on-site for stationary applications or on-board for mobile applications [3].

Currently, steam reforming, partial oxidation and auto thermal reforming of hydrocarbons and alcohols are the major routes for hydrogen production [4]. But all these methods produce a large amount of CO along with hydrogen. CO is a pollutant and poisonous for noble metal catalysts in the electrodes of fuel cell. For all these processes generating hydrogen from these fuels water gas shift (WGS) reaction and preferential oxidation of CO (CO-PROX) would be required to reduce bulk CO and residual CO respectively to an acceptable level from the stream prior to its introduction into fuel cell. Therefore, production of H_2 for PEMFC is usually accomplished by a multistep process that includes catalytic reforming of hydrocarbons and alcohols followed by WGS and CO-PROX. Hence, much attention has been focused on H_2 generation for PEMFC as well as production of CO free hydrogen in recent years [5,6].

Due to the limited activities of current WGS catalysts, approximately 0.5–1 vol.% of unconverted CO still remains in the feed stream and needs to be decreased to a trace level to avoid poisoning of PEMFC anode. CO-PROX appears to be the simplest and most cost effective method to reduce CO concentration in the feed to proton-exchange membrane fuel cells down to few ppm level (<100 ppm) [7]. It is an exothermic process which involves CO oxidation in the reformate stream to CO_2 over a suitable catalyst using molecular O_2. In this respect, previous work from our group has been dedicated to investigate the properties of combinations between copper and cerium oxides (economically favourable formulations in comparison with those, also active, based on noble metals) for CO-PROX reaction [8,9]. On the basis of such works, a new generation of catalysts is being developed in which chemical and structural modifications to the copper oxide component are introduced in order to investigate the effects on the overall CO-PROX performance.

Those previous works have in turn also shown *operando*-infrared (IR) spectroscopy as the most useful tool to explore the catalytic details of redox interfacial activity of those type of catalysts, which constitutes the main basis to achieve details in the

* Corresponding author.
E-mail address: amartinez@icp.csic.es (A. Martínez-Arias).

0920-5861/$ – see front matter © 2009 Elsevier B.V. All rights reserved.
doi:10.1016/j.cattod.2009.08.010

CO oxidation activity, which is the main reaction involved in the whole CO-PROX process [8,9]. In this sense, diffuse reflectance infrared Fourier transform spectroscopy (DRIFTS) has been employed to obtain in situ spectra of the catalysts under reaction condition, employing on line mass spectrometry (MS) analysis to identify and quantify gaseous compounds present in the reaction system. The objective of the present study is to investigate the reactive species of CO-PROX reaction over $(Cu_{0.9}M_{0.1}O)_{0.7}(CeO_2)_{0.3}$ (M = Co, Zn and Sn) catalysts by using mainly such experimental system.

2. Experimental

2.1. Materials

In order to prepare these catalysts by microemulsion method n-heptane, Triton X-100, n-hexanol and tetramethyl ammonium hydroxide (TMAH) were used as organic solvent, surfactant, cosurfactant and precipitation agent, respectively. Required amounts of n-heptane, Triton X-100, and n-hexanol were taken in two conical flasks for two separate microemulsions and they were stirred for 1 h to get a good mixing of the three components. Then required amounts of Cu, Co, Zn and Sn salts solution with water were added into one of two microemulsions. $Cu(NO_3)_2$, $Co(NO_3)_2$, $Zn(NO_3)_2$ and $SnCl_2$ were used as metal precursors. Simultaneously, in another microemulsion of similar characteristics, required amounts of TMAH and water were added. Both microemulsions were kept for another 1 h in agitation with the objective of improving the inlet of the metals and the base into the micelles. After 1 h stirring, the basic microemulsion was introduced into the microemulsion containing the metal precursors in order to precipitate the corresponding metal hydroxides and it was left for the period of 18–24 h under agitation. Then (in the 2nd day), the resulting suspension was heated gently up to 66 °C using a water bath to achieve formation of CuO. During this heating the colour of the mixture changed and a black precipitate could be visible when agitation was stopped after it reached the required temperature. At this point of visible CuO formation, Ce metal salt precursor $Ce(NO_3)_3$ solution with water was added into the Cu-M-containing suspension and kept under stirring for 1 h. After 1 h agitation, the required amount of water dissolved TMAH was added and kept with stirring for the period of 18–24 h to achieve cerium precipitation. Then (in the 3rd day) the solution was finally centrifuged and the solid residue was cleaned with methanol to remove organic solvents, dried at 100 °C for overnight and finally the resulting powders were calcined at 500 °C for 2 h in air. Only for the sample containing Sn, it was washed thoroughly with distilled water to remove chloride ion from the sample. Catalyst samples of $(CuO)_{0.7}(CeO_2)_{0.3}$ and $(Cu_{0.9}M_{0.1}O)_{0.7}(CeO_2)_{0.3}$ [M = Co, Zn and Sn)] are denoted as CuCe, CuCoCe, CuZnCe and CuSnCe respectively.

2.2. Techniques

Quantitative precipitation of Cu, Co, Zn, Sn and Ce cations in these samples has been confirmed by inductively coupled plasma-atomic emission spectroscopy (ICP-AES) chemical analysis.

Specific surface area of the calcined catalysts was determined by BET method from N_2 adsorption isotherms in a Micromeritics 2100 automatic apparatus at liquid nitrogen temperature. The catalysts were degassed at 140 °C in vacuum for 12 h before surface area measurements.

XRD patterns of the samples were recorded on a Seifert XRD 3000P diffractometer using nickel-filtered CuKα radiation operating at 40 kV and 40 mA using a 0.02° step size and 2 s counting time per point. Analysis of the diffraction peaks was done with the computer program ANALYZE Rayflex version 2.293.

Operando-DRIFT spectra of the samples were recorded using a Bruker Equinox 55 FTIR spectrometer equipped with a liquid N_2 cooled high sensitivity MCT detector and a Harrick Praying Mantis DRIFTS cell. All spectra were recorded with an accumulation of 20 scans at a resolution of 4 cm^{-1}. Aliquots of ca. 100 mg catalyst were placed in a sample cup inside the DRIFTS cell with CaF_2 windows and a heating cartridge that allowed samples to be heated up to 500 °C. The DRIFTS cell was connected with a gas handling system in order to measure in situ spectra under controlled gas environments at atmospheric pressure. The samples were activated by in situ calcination for 2 h in a diluted O_2/He stream at 500 °C. Subsequently, the system was cooled down to room temperature and the background spectra were recorded. The reaction mixture (1% CO + 1.25% O_2 + 50% H_2 in He) prepared using mass flow controllers was then passed over the catalysts inside the DRIFTS cell at a total flow rate of 100 cm^3 min^{-1} at atmospheric pressure. The DRIFTS cell was then heated at a rate of 10 °C min^{-1} from room temperature and all spectra were collected typically in every 10 °C interval. Circulating water was used to cool the body of the reaction chamber. As outlet of the DRIFTS cell, a Pfeiffer Omnistar mass spectrometer was connected on line and all corresponding masses were monitored during DRIFTS measurement; note in any case that only qualitative correlations must be intended between DRIFTS results and gases evolutions detected as a consequence of catalytic reactions, taking into account intrinsic limitations of the technique (typically non-differential conditions and limited sampling depth within the catalytic bed). For comparison with the spectra of gaseous CO molecules whose shape changes with the temperature as a consequence of differences in populations of rotational levels, blank runs were done under the same conditions with KBr sample. All the DRIFTS data presented here have accordingly been subtracted from KBr data at each temperature in order to get rid of contribution from CO gas molecules. All spectra obtained were transformed from reflectance units by the use of the Kubelka–Munk function which is linearly related to absorber concentration in DRIFT spectra and referenced to those taken just before CO admission. The CO, O_2 and He used here were supplied by Gas Natural (purity higher than 99.95%).

3. Results and discussion

3.1. Characterization

Chemical analysis for the different components in the present catalysts, as determined by ICP-AES, are displayed in Table 1 indicating the quantitative precipitation of the metals in the respective catalysts. BET surface area values of catalysts are observed to increase generally upon introduction of the second metal compared to parent CuCe and it is highest when CuO is modified with Sn. BET surface areas of all catalysts are shown in Table 2. Fig. 1 displays XRD patterns of the samples. Diffraction peaks attributable to the cubic fluorite phase of CeO_2 are observed in all cases along with several sharp peaks of tenorite CuO phase. There is no indication of presence of Co, Zn or Sn containing phases in the respective XRD pattern of catalysts. Values of CeO_2 lattice

Table 1
Amount of metals determined by ICP-AES for the indicated catalysts.

Catalysts	Ce (wt.%)	Cu (wt.%)	Co (wt.%)	Zn (wt.%)	Sn (wt.%)	Total (%)
CuCe	34.8	38.4				73.2
CuCoCe	39.6	34.1	3.1			76.8
CuZnCe	39.6	34.2		3.5		77.2
CuSnCe	36.2	31.1			3.5	71.8

Table 2
Summary of BET surface area, cell parameters and crystal sizes for the XRD-detected phases in the indicated catalysts.

Catalysts	S_{BET} ($m^2 g^{-1}$)	CeO_2 particle size (nm)	CuO particle size (nm)	CeO_2 cell parameter[a] (Å)	CuO cell parameter[a] (Å)
CuCe	62.98	5.1	16.9	5.391	a = 4.657 b = 3.324 c = 5.111
CuCoCe	78.35	4.6	11.7	5.382	a = 4.689 b = 3.406 c = 5.129
CuZnCe	64.3	3.9	10.9	5.410	a = 4.698 b = 3.424 c = 5.115
CuSnCe	95.48	3.5	22.8	5.377	a = 4.657 b = 3.426 c = 5.111

[a] Estimated errors for the calculations are of ≈±0.048 Å and ≈±0.015 Å for CeO_2 and CuO, respectively.

parameter estimated from the XRD patterns in these CeO_2 coated modified CuO catalysts are, except for CuZnCe, somewhat lower than expected from pure CeO_2 which suggests some incorporation of Cu^{2+} cations into the ceria lattice, taking into account that the radius of Cu^{2+} ions (0.072 nm) is smaller than that of Ce^{4+} ions (0.101 nm). In turn, the lattice parameters for CuO appear slightly larger in these catalysts in comparison with pure CuO [10], which could be due also to some incorporation of the heterometals in the tenorite lattice. Particle size of CeO_2 in CuCe catalyst calculated by Scherrer method is 5.1 nm and decreases to 4.6, 3.9 and 3.5 nm when CuO is doped with Co, Zn and Sn respectively, whereas CuO particle sizes in all catalysts are in the range of 11–23 nm (see Table 2).

3.2. DRIFTS analysis of species formed during CO-PROX reaction

In order to analyse in detail the processes taking place over the catalysts in the course of CO-PROX reaction, the catalysts have been analysed by *operando*-DRIFTS-MS. Figs. 2 and 3 show the DRIFTS results for CuCe and CuCoCe catalysts, respectively, at several reaction temperatures under the CO-PROX mixture; similar results in terms of the bands detected were observed for the other two catalysts (CuZnCe and CuSnCe), as illustrated by Fig. 4 collecting the spectra recorded at a selected temperature. Bands are observed to be basically present in three spectral zones.

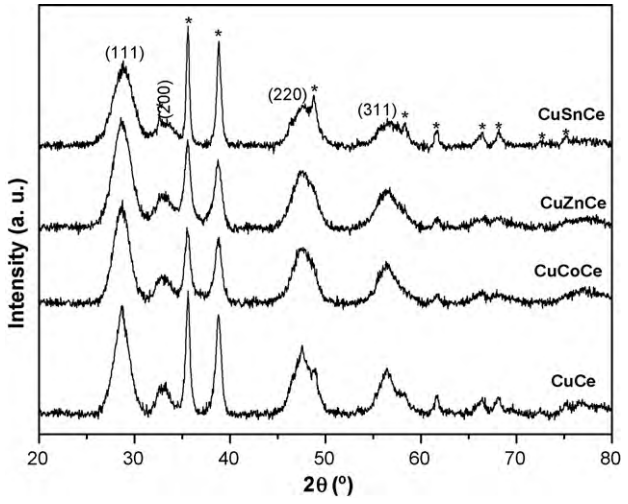

Fig. 1. X-ray diffractograms of CuCe, CuCoCe, CuZnCe and CuSnCe catalysts. Peaks corresponding to tenorite CuO phase are marked with an asterisk and Miller indexes for the fluorite CeO_2 phase are indicated.

A first spectral zone in the 3800–2800 cm^{-1} range (not shown) displays bands mostly attributable to hydroxyl species. In all cases, the spectra are dominated by a broad band extending along this range and displaying a maximum at ca. 3250 cm^{-1}, which is attributable to associated hydroxyl groups affected by hydrogen bonding. Except for CuSnCe, isolated hydroxyl species, expected to yield more or less narrow bands in the 3750–3550 cm^{-1} range [11–13], are practically absent. An increase in the overall hydroxyl intensity, related mainly to increases in associated hydroxyl species, is observed with increasing reaction temperature, in agreement with evolution of the hydrogen oxidation reaction (*vide infra*). The zone between 1800 and 1000 cm^{-1} displays bands mainly attributable to carbonate-type species. Most intense bands in this zone are detected at 1635, 1556, 1468, 1394, 1328 and 1205 cm^{-1}. Bands at 1556 and 1328 cm^{-1} could be attributed to bidentate carbonate, whereas those at 1635, 1394 and 1205 cm^{-1} could be assigned to bicarbonate species that disappears at higher temperature [11]. In turn, the band at 1468 cm^{-1} has been attributed to polydentate carbonate species [12]. No important differences are observed between the samples in this spectral zone except for the relatively higher intensity of bicarbonate species for CuCoCe and CuSnCe (Fig. 4). Formate bands at ca. 1570, 1364 and 2860 cm^{-1}, assignment in accordance with previous work [13], are detected above 180 °C only for CuCoCe (Fig. 3).

Deeper attention is devoted to the intermediate range in which carbonyl species appear, taking into account the high relevancy of the characteristics of such species to explain activity issues in this type of systems [8,9]. The possibility that contributions from electronic transitions in special Ce^{3+} species, which give rise to a relatively broad band in this spectral zone [14], could be overlapped on the carbonyls spectra has been discarded on the basis of fitting work, taking into account similarities encountered between the results observed and recent detailed work in which no hint of such species was detected in a catalyst of this type subjected to ^{12}CO-^{13}CO-TPR-DRIFTS experiments [15]; note also that the reduction degree of the catalyst is expected to increase with temperature under the employed reactant mixture [9] and such Ce^{3+} contribution is not detected at high temperature when no overlapped carbonyls are present as a consequence of their limited thermal stability (Figs. 2 and 3). Fig. 5 displays the spectra obtained under the CO-PROX reaction mixture at 30 °C. Apparent differences between carbonyls formed for each sample are detected. Thus, the spectrum of CuCe is constituted by two bands at 2114 and 2102 cm^{-1}; the presence of two different carbonyls has been also detected in a recent detailed study of a ceria-supported copper oxide catalyst [15]. Two bands are also apparent in the spectra of CuCoCe and CuZnCe. However, for these cases,

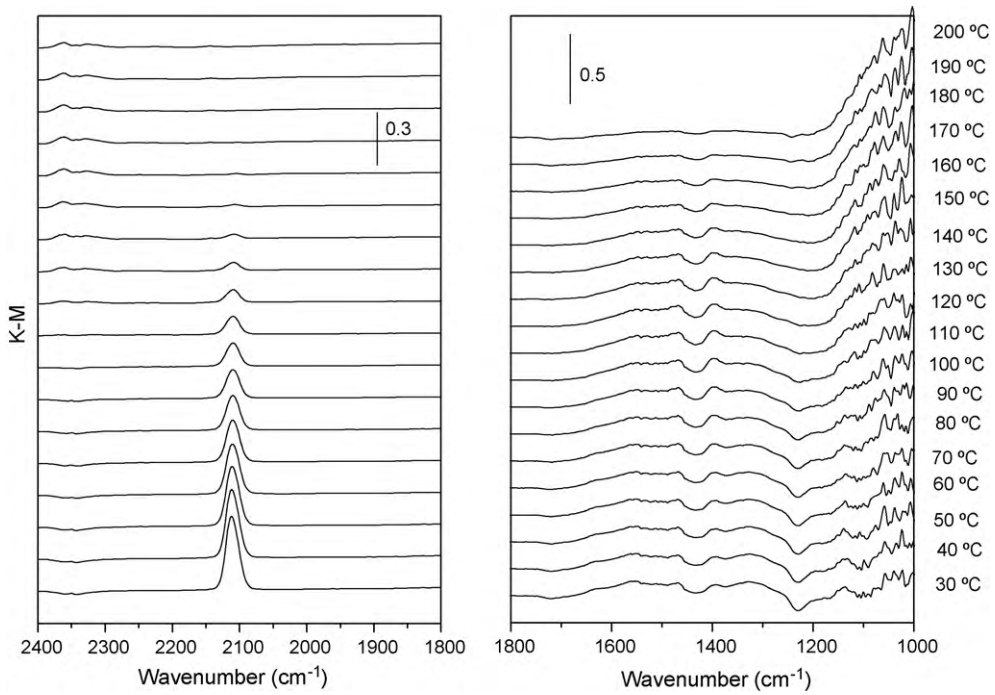

Fig. 2. DRIFTS spectra of several zones recorded during CO-PROX reaction over CuCe catalyst at the indicated temperatures. CO gas contributions were subtracted from the spectra.

they appear slightly blue-shifted to 2121 and 2107 cm^{-1} while they are broader, particularly in the latter case, than for CuCe. In turn, the spectrum of CuSnCe displays relatively broad bands at 2123 and 2107 cm^{-1} as well as a very broad third component centred at 2089 cm^{-1}. Bands at 2123–2114 cm^{-1} are attributed to Cu^{+}-carbonyl species on the basis of previous works, taking into account their relatively high thermal stability as well as isotopic shifts detected in ^{12}CO- vs. ^{13}CO-TPR experiments [8,9,15]. Some doubts may arise concerning the nature of the bands at 2107–2102 cm^{-1}. Since their relatively low frequency suggests that they may be related to metallic copper carbonyls, recent experiments displayed thermal stabilities for this type of bands similar to those observed for the Cu^{+}-carbonyl species appearing at higher frequency, suggesting that the adsorption centre could also correspond to partially oxidised copper species. Indeed, an independent CO-TPD-DRIFTS experiment performed over CuCe did not show important differences between thermal stabilities of both carbonyls, only slightly higher for the one at higher

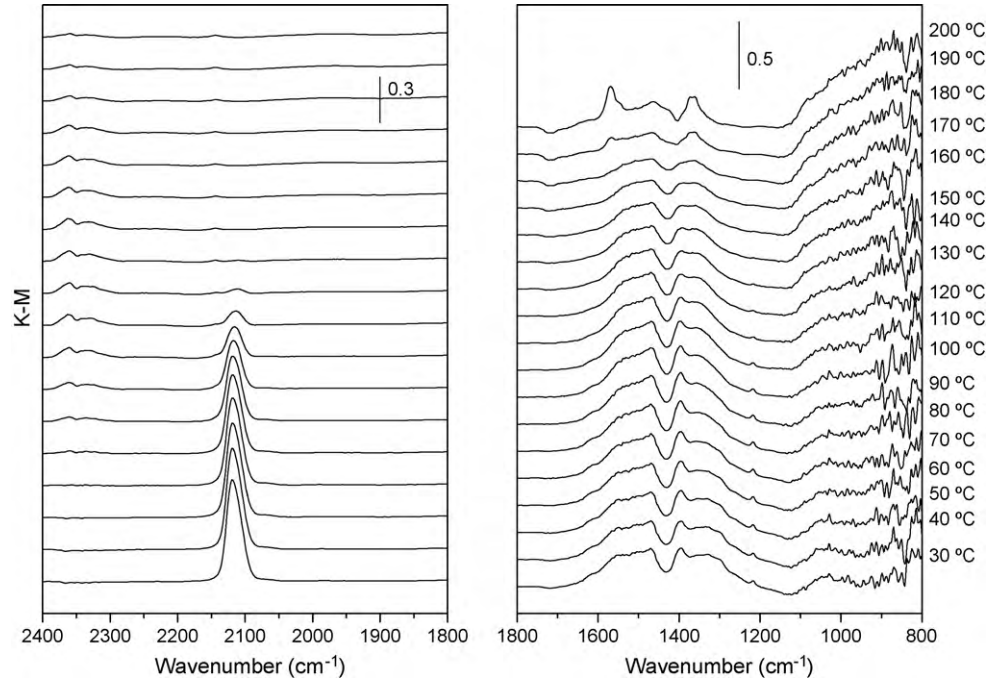

Fig. 3. The same as Fig. 2, for the CuCoCe catalyst.

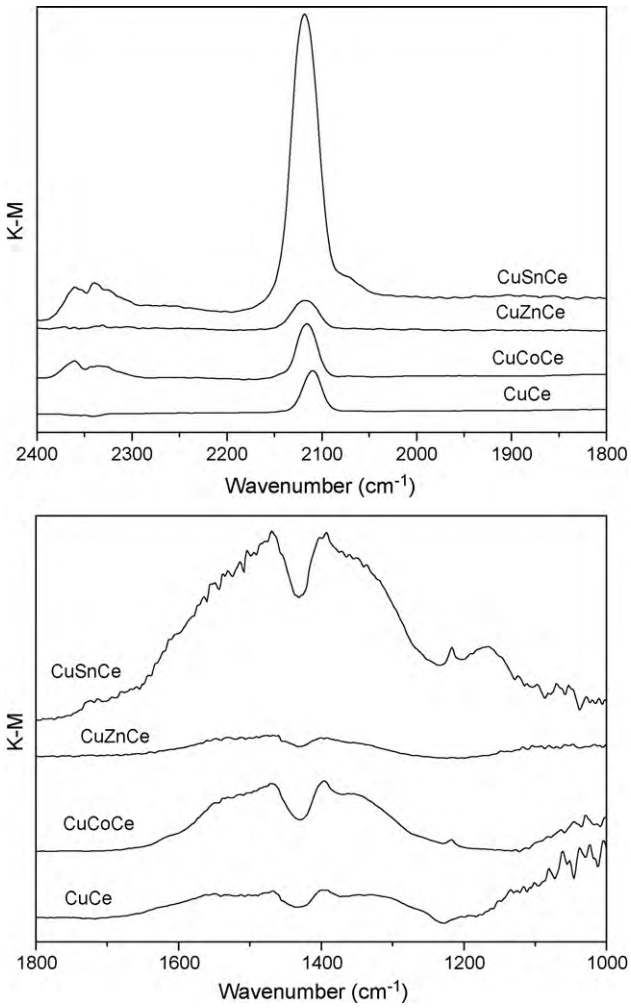

Fig. 4. DRIFTS spectra recorded under the CO-PROX mixture over the indicated catalysts at 100 °C.

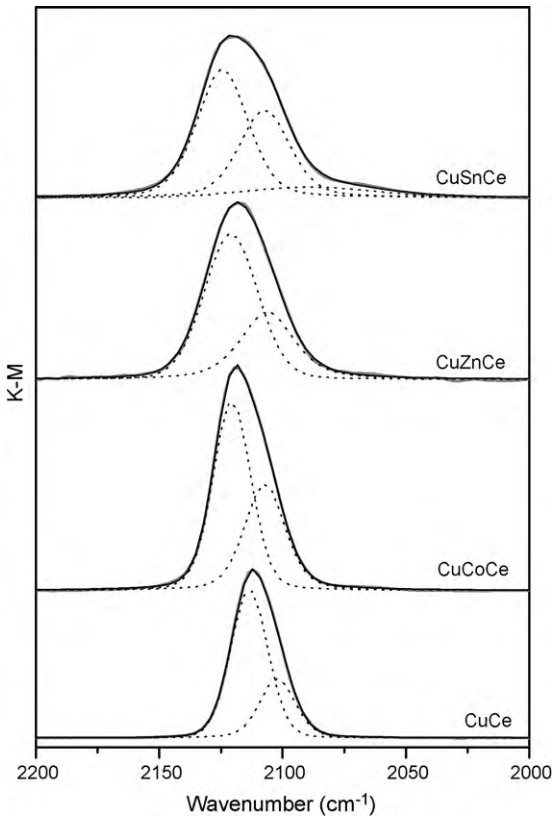

Fig. 5. DRIFTS spectra and fittings in the zone corresponding to carbonyl species for the indicated samples under CO-PROX conditions at 30 °C.

frequency, suggesting that Cu^+ centres could be as well a reasonable attribution for the adsorption sites of the low frequency carbonyls, Fig. 6; it must be noted in this sense that metallic copper carbonyls are typically very easily eliminated upon room temperature purging under inert gas [16]. The same holds for carbonyls detected in the samples doped with a second metal, which display thermal stabilities for the two carbonyls similar to those detected for the CuCe sample; Fig. 7 displays these experiments for the CuCoCe sample as a representative example. Since in any case ceria interaction with the copper adsorption sites must be invoked in order to explain the red shift with respect to similar bands detected in pure Cu_2O [8,9,15,17], the presence of the two types of carbonyls reveals at least two different types of copper sites in the catalysts, subjected to a different degree of interaction with the ceria component. In turn, the blue shift detected in the two carbonyls in the presence of Co, Zn or Sn suggests some modification of such interaction in the presence of such metals. In any case, the relatively strong red shift detected for this type of Cu^+-carbonyls in comparison with those detected in Cu_2O [17], along with their relatively strong resistance towards desorption, suggests a strong π-back bond component in them, according to usual σ bond-π-back bond scheme employed to explain carbonyl bonds in this type of species [17–19]. On the other hand, the carbonyl at 2089 cm^{-1} may well correspond to a metallic copper carbonyl, given its relatively low frequency [16–19]. Note in this sense that carbonyls formed on oxidised tin centres are expected to give rise to bands at appreciably higher frequency [20].

3.3. MS analysis of gases evolved during CO-PROX reaction

Fig. 8 displays changes of different gases monitored during CO-PROX reaction over all catalysts studied here. Even though catalytic activities appear relatively close to one another, there are some subtle differences in CO as well as H_2 oxidation features in these catalysts if we look at carefully. In cases of CuSnCe and CuCoCe, CO oxidation starts at 50 °C continuing the CO_2 production up to 200 and 190 °C and after this temperature, H_2 oxidation predominates over CO oxidation, as revealed by the H_2O production evolution. Therefore, in these cases, CO-PROX window is in between 50–200 and 50–190 °C, respectively. On the other hand, this window is between ca. 65 and 250 °C for CuZnCe and CuCe catalysts. CO_2 and H_2O production characteristics are also reflected in O_2 consumption profiles. Note there are two steps in O_2 consumption corresponding to CO and H_2 oxidation, respectively. It is clear that O_2 consumption for H_2O production due to H_2 oxidation occurs at slightly lower temperature for CuSnCe and CuCoCe compared to other two catalysts, as also reflected by respective H_2O evolutions. On the other hand, O_2 consumption completed within 225 °C over CuSnCe and CuCoCe, whereas O_2 consumption apparently levels off at higher temperature on CuZnCe and CuCe catalysts. In addition, CH_4 formation through methanation reaction ($CO + 3H_2 \rightarrow CH_4 + H_2O$) has been detected only in the case of CuCoCe catalyst above ca. 250 °C (not shown), in agreement with literature results displaying such activity in the presence of cobalt [21]. It may also be noted some irregularity in the profiles of CO_2 evolution with several relative maxima appearing in some case, not directly correlated with CO evolution. This somewhat differs

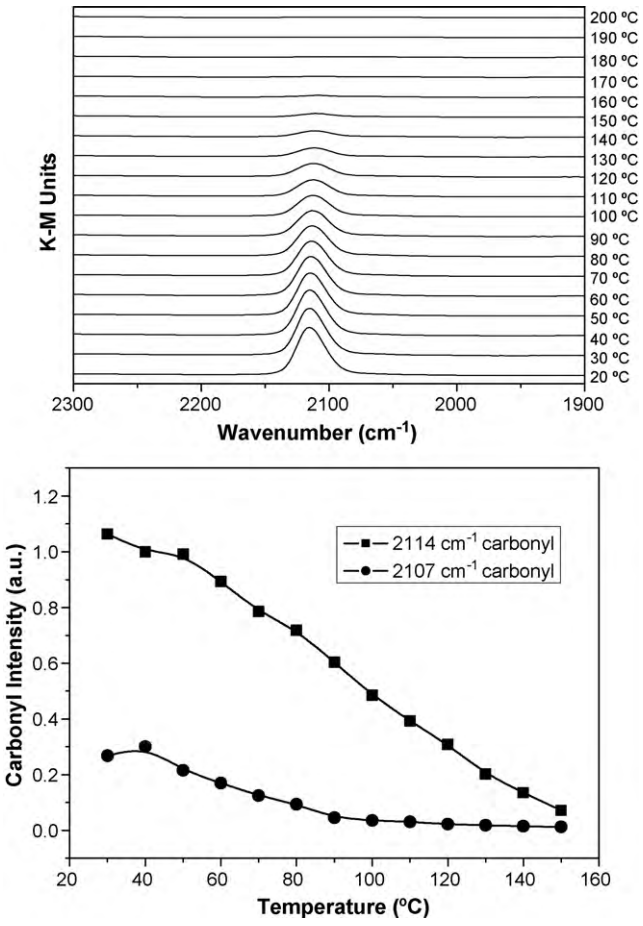

Fig. 6. Top: DRIFTS spectra after introduction of a flow of diluted CO at 30 °C over calcined CuCe followed by desorption under flowing inert gas at the indicated temperatures. Bottom: evolution of the two detected carbonyls as a function of desorption temperature.

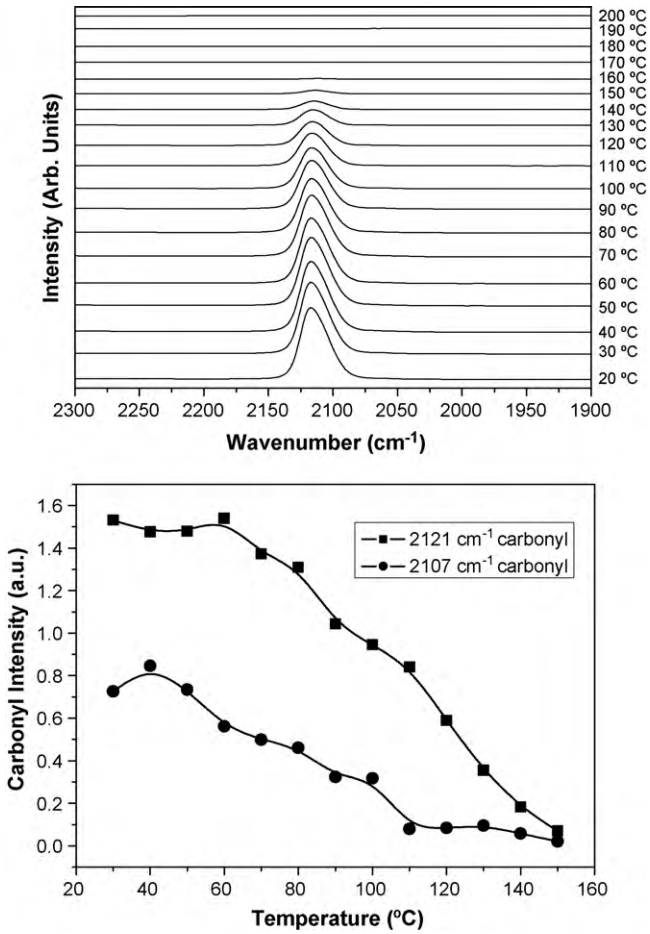

Fig. 7. The same as Fig. 6, for the CuCoCe sample.

from previous experience on other catalysts of this type, in which the spectra were collected under isothermal steady-state conditions [8], and suggests the presence to some extent of overlapping effects of carbonate decomposition on these profiles. Nevertheless, it must be noted that main conclusions are taken on the basis of respective CO evolutions, expected to be less affected by such effects.

Previous in situ DRIFTS-MS studies from our group have demonstrated that CO preferential oxidation on these type of catalysts depends on the magnitude of initial interfacial reductive process occurred in $CuO–CeO_2$ interface at low temperature (typically room temperature), whereas H_2 oxidation activity is related to the propagation of the reduction to the rest (far from the interface, less affected by interactions with ceria) of the CuO particles present in the catalyst [9]. Such low temperature interfacial reduction process is not apparent in the reactions done in classical reactors due either to having taken place during initial gas equilibration (being difficult to separate from gas concentration oscillations due to valve openings and so on) or because it involves a relatively low amount of the whole copper, strictly related to $CuO–CeO_2$ interfacial sites [8,9]. In our present study, DRIFTS results show the formation of Cu^+ species along with carbonates already upon introduction of the CO-PROX mixture over the catalysts at 30 °C, Figs. 2, 3 and 5. As observed during similar experiments over other catalysts of this type [8,9], this indicates a low temperature process involving the initial reduction of interfacial CuO sites. According to those previous investigations [9], the magnitude of this low temperature interfacial reductive process determines the activity of CO oxidation, strongly suggesting in turn that active sites for such reaction are related to partially reduced CuO particles with the role of ceria being mainly related to promotion of such low temperature reduction process [9]. This appears also in qualitative agreement with results observed in this case, according to the intensities of Cu^+-carbonyls detected for the different catalysts, Fig. 9, showing relatively higher intensity for most active CuSnCe and CuCoCe catalysts. Therefore, on the basis of the analysis of the characteristics of the copper carbonyl species formed in each case, it appears that their relative intensity is one of the main factors to explain the CO oxidation activity achieved while other electronic effects that must be involved in respective shifts detected (Fig. 5) would be of lesser importance. On the other hand, activity results for the H_2 oxidation reaction suggests that, considering previous hypotheses [9], propagation of copper oxide reduction is most favoured for most active CuCoCe and CuSnCe samples. Details for such process are however not easily inferred from evolution of the copper carbonyls formed in the course of the reaction, given the relatively higher temperature at which this reaction onsets, which prevents observation of carbonyl species mainly as a consequence of their thermal stability (Fig. 6). In this sense, correlation with copper oxide particle size (Table 1), considering that smaller particles are expected to be more reducible in this type of systems [8], and as a consequence more active for H_2 oxidation, could not be established either. Nevertheless, a correlation is observed between hydrogen oxidation activity

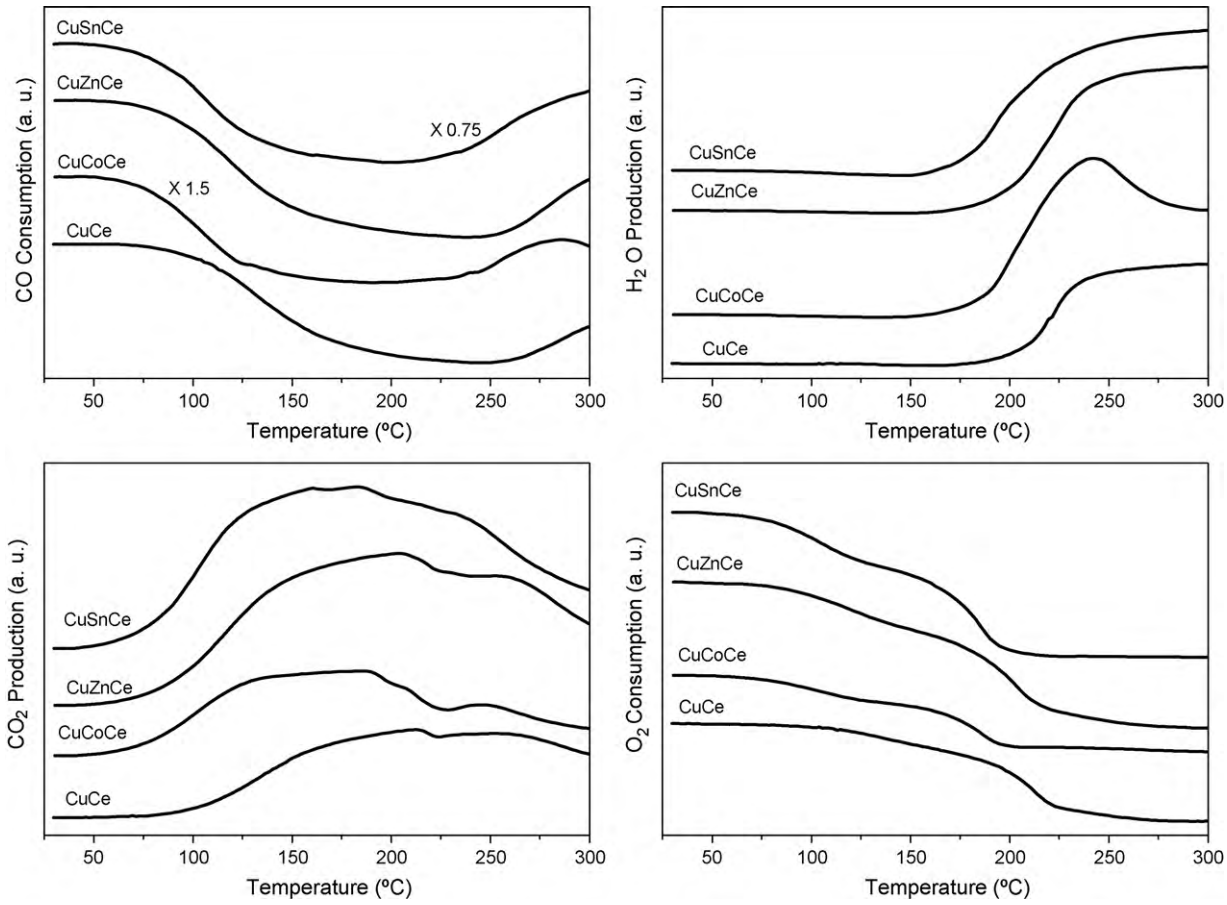

Fig. 8. Evolution of the indicated gases during the course of the CO-PROX reaction performed with the DRIFTS cell over the indicated samples.

and the relative intensity of the lowest frequency Cu^+-carbonyl species (band at 2107–2102 cm^{-1}). Thus, the intensity ratio between this carbonyl and the highest frequency one (at 2123–2114 cm^{-1}) is appreciably higher, considering spectra taken at the lowest reaction temperature, for most active CuCoCe and CuSnCe samples (0.57 and 0.70, respectively) than for the least active ones (0.40 and 0.43 for CuCe and CuZnCe, respectively). This suggests that such type of sites in which electron transfer processes from ceria would be most favoured, likely favouring in turn their overall reducibility, could provide sites most active for such reaction within this type of catalysts.

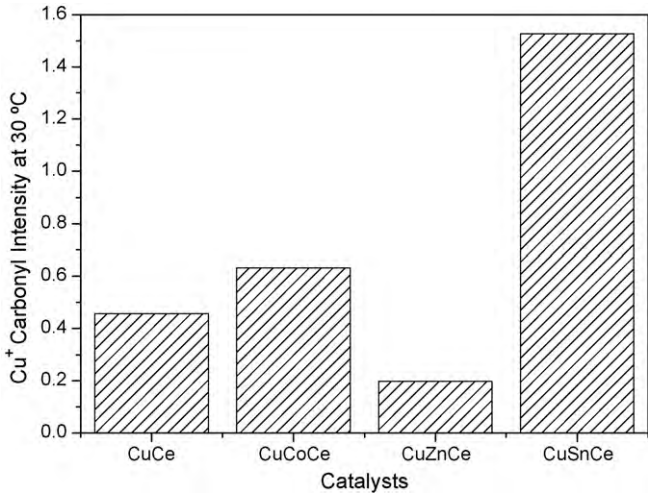

Fig. 9. Intensities of carbonyls detected under CO-PROX conditions at 30 °C for the indicated catalysts.

4. Conclusions

Catalysts prepared by microemulsion and involving combination of copper and cerium oxides in which the former has been modified by incorporation of Co, Zn or Co has been examined with respect to their activity and redox properties under CO-PROX conditions by means of *operando*-DRIFTS-MS. Carbonyl and carbonate-type species are evidenced to be formed at low temperature upon contact of the catalysts with the reaction mixture, revealing the existence of a reductive process whose magnitude basically determines the CO oxidation activity of the systems. Nevertheless, differences are detected in the nature of two main Cu^+-carbonyl species formed in each case as revealed by shifts observed in their frequencies as a function of the presence of the mentioned dopants, which appear of lesser relevancy to explain catalytic properties for CO oxidation under CO-PROX conditions in this type systems. In turn, relative intensities of the mentioned two Cu^+-carbonyl species could provide hints to explain differences in H_2 oxidation activities under CO-PROX conditions.

Acknowledgements

P.B. is thankful to 6th European Community Framework Programme for a Marie Curie Incoming International Fellowship. A.H. and A.L.C. thank the Ministerio de Ciencia e Innovación and CSIC, respectively, for FPU and JAE PhD grants under which their contribution to this work was carried out. Financial support by

MEC Plan Nacional (project CTQ2006-15600/BQU) and Comunidad de Madrid (project ENERCAM S-0505/ENE/000304) is acknowledged.

References

[1] J.R. Rostrup-Nielsen, Phys. Chem. Chem. Phys. 3 (2001) 283.
[2] J.A. Turner, Science 305 (2004) 972.
[3] L.F. Brown, Int. J. Hydrogen Energy 26 (2001) 381.
[4] P. Ferreira-Aparicio, M.J. Benito, J.L. Sanz, Catal. Rev. Sci. Eng. 47 (2005) 491.
[5] C. Song, Catal. Today 77 (2002) 17.
[6] T.V. Choudhary, D.W. Goodman, Catal. Today 77 (2002) 65.
[7] R.J. Farrauto, Y. Liu, W. Ruettinger, O. Ilinich, L. Shore, T. Giroux, Catal. Rev. Sci. Eng. 49 (2007) 141.
[8] D. Gamarra, G. Munuera, A.B. Hungria, M. Fernández-García, J.C. Conesa, P.A. Midgley, X.Q. Wang, J.C. Hanson, J.A. Rodriguez, A. Martínez-Arias, J. Phys. Chem. C 111 (2007) 11026.
[9] D. Gamarra, C. Belver, M. Fernández–García, A. Martínez-Arias, J. Am. Chem. Soc. 129 (2007) 12064.
[10] X. Wang, J.A. Rodriguez, J.C. Hanson, D. Gamarra, A. Martínez-Arias, M. Fernández-García, J. Phys. Chem. B 109 (2005) 19595.
[11] C. Binet, A. Badri, J.-C. Lavalley, J. Phys. Chem. 98 (1994) 6392.
[12] C. Binet, M. Daturi, J.-C. Lavalley, Catal. Today 50 (1999) 207.
[13] C. Li, Y. Sakata, T. Arai, K. Domen, K.-I. Maruya, T. Onishi, J. Chem. Soc. Faraday Trans. I 85 (1989) 1451.
[14] H. Daly, J. Ni, D. Thompsett, F.C. Meunier, J. Catal. 254 (2008) 238.
[15] P. Bera, A. López Cámara, A. Hornés, A. Martínez-Arias, J. Phys. Chem. C 113 (2009) 10689.
[16] M.B. Padley, C.H. Rochester, G.J. Hutchings, F. King, J. Catal. 148 (1994) 438.
[17] D. Scarano, S. Bordiga, C. Lamberti, G. Spoto, G. Ricchiardi, A. Zecchina, C. Otero Areán, Surf. Sci. 411 (1998) 272.
[18] P. Hollins, Surf. Sci. Rep. 16 (1992) 53.
[19] K.I. Hadjiivanov, M. Kantcheva, D.G. Klissurski, J. Chem. Soc. Faraday Trans. 92 (1996) 4595.
[20] D. Amalric-Popescu, F. Bozon-Verduraz, Catal. Lett. 64 (2000) 125.
[21] A.A. Firsova, T.I. Khomenko, A.N. Il'ichev, V.N. Korchak, Kinet. Catal. 49 (2008) 682.